

# Adjusted Random Effect Block Bootstraps for Highly Unbalanced Clustered Data

Zhi Yang Tho\*, Raymond Chambers, and A.H. Welsh

Research School of Finance, Actuarial Studies and Statistics, The Australian National University, Australia

## Abstract

Clustered data arise naturally in many scientific and applied research settings where units are grouped within clusters. They are commonly analyzed using linear mixed models to account for within-cluster correlations. This article focuses on the scenario in which cluster sizes might be highly unbalanced and proposes a proportional random effect block bootstrap and a modified random effect block bootstrap, which are applicable in such cases and accommodate general distributions of random effects and error terms. These methods generalize the random effect block bootstrap, originally designed for the balanced case, and can be used for inference on parameters of linear mixed models or functions thereof. Both proposed bootstraps are shown to enjoy Fisher consistency under general cluster sizes, while the original random effect block bootstrap is consistent only for balanced clusters. Simulations demonstrate strong finite sample inferential performance of the proposed bootstraps relative to the random effect block bootstrap and other existing bootstrap methods for clustered data. Application to the Oman rainfall enhancement trial dataset, with cluster sizes ranging from 1 to 58, shows improved bootstrap confidence intervals using the proposed bootstraps over the random effect block bootstrap and a statistically significant effect of the ionization technology on rainfall.

*Keywords:* Confidence interval; Linear mixed model; Non-normal data; PPS sampling; Unbalanced data; Variance components.

---

\*Corresponding author: ZhiYang.Tho@anu.edu.au; Research School of Finance, Actuarial Studies and Statistics, The Australian National University, Canberra, ACT 2600, Australia.

# 1 Introduction

The bootstrap was introduced by [Efron \(1979\)](#) as a method to estimate the sampling distribution of a statistic of interest. The bootstrap procedure, originally designed for independent and identically distributed (i.i.d.) data, involves drawing random samples with replacement from the observed data and computing the statistic for each bootstrap sample. The empirical distribution of these bootstrapped statistics is then used to approximate the sampling distribution of the original statistic. A key advantage of the bootstrap is its flexibility in dealing with complicated statistics without requiring strong distributional assumptions. As a result, the bootstrap has been extensively studied and applied to a wide range of statistical problems (e.g., [Efron and Tibshirani, 1994](#); [Hall, 1992](#); [Davison and Hinkley, 1997](#)).

The bootstrap has also been extended beyond the independent data setting to dependent data such as time series and spatial data. In time series analysis, different variants of the block bootstrap are used to account for the underlying serial dependence structure by resampling blocks of observations rather than individual data points (see e.g., [Künsch, 1989](#); [Pilavakis et al., 2019](#)). Alternatively, [Bühlmann \(1997\)](#) and [Friedrich and Lin \(2024\)](#), among others, studied sieve bootstraps which involve resampling the residuals from estimated autoregressive models. A block bootstrap method has also been applied to spatially dependent data ([Lahiri and Zhu, 2006](#)). Another approach to bootstrapping spatial data involves removing the underlying spatial correlation before resampling the resulting uncorrelated data ([Castillo-Páez et al., 2019](#)).

In this article, we focus on bootstrap procedures for a specific type of dependent data, namely clustered data, in which observations are grouped into known clusters. Clustered data commonly arise in various fields, such as healthcare where patients are grouped by hospitals, education where students are grouped by schools, and economics where firms are grouped by industries. A popular method for analyzing such data is the linear mixed model ([Pinheiro and Bates, 2000](#); [Bates et al., 2015](#)), which incorporates fixed effects to capture population-level effects and random

effects to account for within-cluster dependence and between-cluster variability. Various bootstrap methods designed to account for the underlying dependence structure of clustered data have been proposed for inference on the parameters of the linear mixed model. [Davison and Hinkley \(1997\)](#) and [McCullagh \(2000\)](#) proposed several variations of the cluster bootstrap, where clusters are randomly sampled with replacement, followed by optional random permutation or resampling of observations within clusters. Motivated by the generalized bootstrap of [Chatterjee and Bose \(2005\)](#), [Field et al. \(2010\)](#) and [O'Shaughnessy and Welsh \(2018\)](#) studied the generalized cluster bootstrap which involves resampling weights for the corresponding estimating equations.

Another bootstrap approach for clustered data, commonly referred to as residual bootstrap or random effect bootstrap, involves resampling predictors of residuals and/or random effects. [Butar and Lahiri \(2003\)](#) and [Kubokawa and Nagashima \(2012\)](#) considered parametric versions of such bootstraps, where the residuals and random effects are sampled from normal distributions with the corresponding estimated variance components. However, the validity of the parametric bootstrap is highly dependent upon the stochastic assumption of the model e.g., the normality assumption of random effects. To overcome this, semiparametric version of the random effect/residual bootstraps have been considered (see e.g., [Carpenter et al., 2003](#); [Chambers and Chandra, 2013](#); [Reluga et al., 2024](#), among others). Of particular note is the semiparametric random effect block (REB) bootstrap of [Chambers and Chandra \(2013\)](#) that involves resampling cluster-level random effect predictors, along with sampling clusters (“blocks”) followed by resampling residuals within the sampled clusters.

For clustered data with highly unbalanced cluster sizes, e.g., some clusters have only one observation while other clusters have more than, say, 50 observations, this article proposes a proportional random effect block (PREB) bootstrap and a modified version of the REB bootstrap. This is motivated by the Oman rainfall enhancement trial data in Section 5, where positive rainfall amounts are observed at 1–58 precipitation gauges clustered within days, so the clusters vary in size

from 1–58 gauges. While various bootstraps have been proposed for clustered data as reviewed above, there are very limited studies that specifically investigate the impact of highly unbalanced cluster sizes on the bootstrap performance. The only exception is [Samanta and Welsh \(2013\)](#) who concluded that the generalized cluster bootstrap performs better than the transformation bootstrap in approximating the sampling distribution and sampling variance of fixed effect and variance component estimators. However, to our knowledge, there is no study that has considered the impact of highly unbalanced cluster sizes on bootstrap inferential performance e.g., coverage of bootstrap confidence intervals for parameters of linear mixed models. Given the importance of bootstraps in conducting inferences ([Efron and Tibshirani, 1994](#); [Davison and Hinkley, 1997](#)), this article endeavours to bridge this gap in the literature.

The proposed bootstraps are generalizations of the REB bootstrap of [Chambers and Chandra \(2013\)](#) that implicitly assumed balanced cluster sizes. The core idea of the PREB and modified REB bootstraps is to apply appropriate centering and/or scaling to the random effect and residual predictors before resampling with a suitable sampling scheme for the unbalanced clusters. We prove the Fisher consistency of the proposed bootstraps under both balanced and highly unbalanced cluster sizes, and show that the REB bootstrap is only consistent for the balanced case. Simulation studies demonstrate that the proposed bootstraps outperform the REB bootstrap in terms of empirical coverage of bootstrap confidence intervals when cluster sizes are highly unbalanced, and that they also perform better than other commonly used bootstraps, e.g., the parametric bootstrap, when the simulated random effects and error terms are non-normal. To the best of our knowledge, this is among the first studies to provide a direct comparison of the inferential performance of random effect bootstraps, motivated by linear mixed models, with other general bootstraps designed for clustered data such as the cluster bootstrap and the generalized cluster bootstrap. An application of the PREB and modified REB bootstraps to the Oman rainfall enhancement trial data reinforces the value of the proposed bootstraps over the REB bootstrap, as the confidence

intervals of the variance components using the latter bootstrap perform poorly.

The rest of this article is organized as follows. Section 2 introduces the linear mixed model and the proposed PREB and modified REB bootstraps. Section 3 presents theoretical results for the proposed bootstraps under general cluster sizes and compares them to the REB bootstrap. Section 4 presents results of a simulation study, while an application to the Oman rainfall enhancement trial data is provided in Section 5. Section 6 offers some concluding remarks.

## 2 Linear Mixed Model and Adjusted REB Bootstraps

Let  $y_{ij}$  denote the response and  $\mathbf{x}_{ij} = (1, x_{ij,1}, \dots, x_{ij,p-1})^\top$  denote the  $p$ -dimensional covariate vector of unit  $j$  in cluster  $i$  for  $j = 1, \dots, n_i$  and  $i = 1, \dots, D$ . That is, there are  $D$  clusters with cluster sizes  $n_i$ , and  $N = \sum_{i=1}^D n_i$  total observations. We will discuss the properties of the bootstraps under two cases: (i) balanced cluster sizes where  $n_i = N/D$  for all  $i = 1, \dots, D$ ; and (ii) highly unbalanced cluster sizes where  $n_i$  may vary from one to, say, 50 or more.

Clustered data of this form are commonly modeled with linear mixed models to account for different sources of variation. In this article, we focus on the linear random intercept model

$$y_{ij} = \mathbf{x}_{ij}^\top \boldsymbol{\beta} + u_i + e_{ij}, \quad \text{for } j = 1, \dots, n_i, \quad i = 1, \dots, D, \quad (1)$$

where  $\boldsymbol{\beta} = (\beta_0, \dots, \beta_{p-1})$  is the vector of fixed effects,  $u_i$  are i.i.d. cluster-level random effects with mean 0 and variance  $\sigma_u^2$ , and  $e_{ij}$  are i.i.d. unit-level error terms with mean 0 and variance  $\sigma_e^2$ . The random effects are assumed to be independent of the error terms, and normality is not required for our bootstrap methods. Furthermore, model (1) can be written in an equivalent vector form as

$$\mathbf{y} = \mathbf{X}\boldsymbol{\beta} + \mathbf{Z}\mathbf{u} + \mathbf{e},$$

where  $\mathbf{y} = (\mathbf{y}_1^\top, \dots, \mathbf{y}_D^\top)^\top$  is the  $N$ -dimensional vector of stacked responses,  $\mathbf{y}_i = (y_{i1}, \dots, y_{in_i})^\top$ ,  $\mathbf{X} = (\mathbf{X}_1^\top, \dots, \mathbf{X}_D^\top)^\top$  is the  $N \times p$  fixed effect model matrix,  $\mathbf{X}_i = (\mathbf{x}_{i1}, \dots, \mathbf{x}_{in_i})^\top$ ,  $\mathbf{Z} = \text{diag}(\mathbf{1}_{n_1}, \dots, \mathbf{1}_{n_D})$  is the  $N \times D$  block diagonal random effect model matrix with block  $i$  given by the  $n_i$ -dimensional vector of ones  $\mathbf{1}_{n_i}$ ,  $\mathbf{u} = (u_1, \dots, u_D)^\top$  is the  $D$ -dimensional vector of stacked random intercepts,  $\mathbf{e} = (e_1^\top, \dots, e_D^\top)^\top$  is the  $N$ -dimensional vector of stacked errors, and  $\mathbf{e}_i = (e_{i1}, \dots, e_{in_i})^\top$ . This leads to  $\mathbb{E}(\mathbf{y}) = \mathbf{X}\beta$  and  $\text{var}(\mathbf{y}) = \Sigma(\sigma_u^2, \sigma_e^2) = \sigma_u^2 \mathbf{Z} \mathbf{Z}^\top + \sigma_e^2 \mathbf{I}_N$ , where the variance reflects correlations within clusters. The fixed effects  $\beta$  capture the systematic impact of covariates on the response, whereas the variance components  $\sigma_u^2$  and  $\sigma_e^2$  measure between-cluster variability and within-cluster variability, respectively. These parameters and their estimators are denoted as  $\theta = (\beta^\top, \sigma_u^2, \sigma_e^2)^\top$  and  $\hat{\theta} = (\hat{\beta}^\top, \hat{\sigma}_u^2, \hat{\sigma}_e^2)^\top$ , respectively, where  $\hat{\theta}$  are typically obtained via the maximum likelihood (ML) or restricted maximum likelihood (REML) approach (Patterson and Thompson, 1971; Harville, 1977; Bates et al., 2015), assuming a Gaussian working likelihood. For example, the ML estimator is defined as the maximizer of

$$l(\theta; \mathbf{y}, \mathbf{X}) = \sum_{i=1}^D l_i(\theta; \mathbf{y}_i, \mathbf{X}_i) = \frac{1}{2} \log |\Sigma^{-1}(\sigma_u^2, \sigma_e^2)| - \frac{1}{2} (\mathbf{y} - \mathbf{X}\beta)^\top \Sigma^{-1}(\sigma_u^2, \sigma_e^2) (\mathbf{y} - \mathbf{X}\beta),$$

where  $l(\theta; \mathbf{y}, \mathbf{X})$  and  $l_i(\theta; \mathbf{y}_i, \mathbf{X}_i)$  are the log-likelihood of  $\mathbf{y}$  and  $\mathbf{y}_i$ , respectively, ignoring some constants. Marginal residuals  $r_{ij} = y_{ij} - \mathbf{x}_{ij}^\top \hat{\beta}$  can be computed, and used to obtain the cluster-level random effect predictors and unit-level residuals as

$$\hat{u}_i = \frac{1}{n_i} \sum_{j=1}^{n_i} r_{ij} \text{ and } \hat{e}_{ij} = r_{ij} - \hat{u}_i, \quad (2)$$

respectively, for  $j = 1, \dots, n_i$  and  $i = 1, \dots, D$ . These quantities,  $\hat{u}_i$  and  $\hat{e}_{ij}$ , form the basis of our bootstrap procedures;  $\hat{u}_i$  is a rescaled (unshrunk) version of the usual empirical best linear unbiased predictors (EBLUPs). We describe a prescaled proportional random effect block (PREB)

bootstrap and a modified random effect block (REB) bootstrap in the following subsections. The methods are applicable to both balanced and highly unbalanced clusters, and are inspired by the REB bootstrap of [Chambers and Chandra \(2013\)](#) which required balanced clusters.

## 2.1 Prescaled PREB Bootstrap

The prescaled PREB (PREB-1) bootstrap employs the idea of “reflating” introduced by [Carpenter et al. \(2003\)](#) to “unshrink” EBLUPs, by centering and scaling the cluster-level random effects  $\hat{u}_i$  and unit-level residuals  $\hat{e}_{ij}$ : set  $\hat{u}_i^c = \hat{u}_i - D^{-1} \sum_{i'=1}^D \hat{u}_{i'}$  and compute

$$\hat{u}_i^{sc} = \hat{u}_i^c \frac{\hat{\sigma}_u}{\sqrt{D^{-1} \sum_{i'=1}^D (\hat{u}_{i'}^c)^2}}, \quad \hat{e}_{ij}^s = \hat{e}_{ij} \frac{\hat{\sigma}_e}{\sqrt{N^{-1} \sum_{i'=1}^D \sum_{j'=1}^{n_{i'}} \hat{e}_{i'j'}^2}}, \quad (3)$$

for  $j = 1, \dots, n_i$  and  $i = 1, \dots, D$ . Let  $\text{SRSWR}(\mathbf{a}, c)$  denote  $c$  independent draws from the vector  $\mathbf{a}$  using simple random sampling (SRS) with replacement and  $\text{PPSWR}(\mathbf{a}, \mathbf{b}, c)$  denote  $c$  independent draws from  $\mathbf{a} = (a_1, \dots, a_D)$  using probability-proportional-to-size (PPS) sampling with replacement with probabilities proportional to  $\mathbf{b} = (b_1, \dots, b_D)$ , i.e., the selection probability of  $a_i$  is  $b_i / \sum_{i'=1}^D b_{i'}$ . The full PREB-1 bootstrap procedure is described in [Algorithm 1](#).

The bootstrap distributions for different elements of  $\hat{\theta}$  obtained from [Algorithm 1](#) can be used to form bootstrap confidence intervals for the corresponding elements of the parameter vector  $\theta$ . While many methods can be used to form such intervals (see e.g., [Efron and Tibshirani, 1994](#); [Davison and Hinkley, 1997](#)), this article concentrates on the bootstrap percentile confidence intervals. Under this method, a  $100(1 - \alpha)\%$  confidence interval for the  $k$ -th element of  $\theta$  (denoted  $\theta_k$ ) is constructed as  $(\hat{\theta}_{k,\alpha/2}^*, \hat{\theta}_{k,1-\alpha/2}^*)$ , where  $\hat{\theta}_{k,\alpha/2}^*$  and  $\hat{\theta}_{k,1-\alpha/2}^*$  denote the  $\alpha/2$  and  $1 - \alpha/2$  quantiles of the bootstrap distribution for  $\hat{\theta}_k$ , respectively, and  $\hat{\theta}_k$  denotes the  $k$ -th element of  $\hat{\theta}$  for  $k = 1, \dots, p + 2$ .

While the marginal residuals  $r_{ij}$  are generated from the fixed effect structure of the model, the

---

**Algorithm 1:** Algorithm for the PREB-1 bootstrap.

---

**Input:** ML or REML estimates  $\hat{\theta} = (\hat{\beta}^\top, \hat{\sigma}_u^2, \hat{\sigma}_e^2)^\top$ .

1. Compute marginal residuals  $\mathbf{r}_i = (r_{i1}, \dots, r_{in_i})^\top = \mathbf{y}_i - \mathbf{X}_i \hat{\beta}$  for  $i = 1, \dots, D$ . Obtain cluster-level random effect predictors  $\hat{\mathbf{u}} = (\hat{u}_1, \dots, \hat{u}_D)^\top$  and unit-level residuals  $\hat{\mathbf{e}}_i = (\hat{e}_{i1}, \dots, \hat{e}_{in_i})^\top$  from (2).
2. Reflate these quantities to  $\hat{\mathbf{u}}^{sc} = (\hat{u}_1^{sc}, \dots, \hat{u}_D^{sc})^\top$  and  $\hat{\mathbf{e}}_i^s = (\hat{e}_{i1}^s, \dots, \hat{e}_{in_i}^s)^\top$  for  $i = 1, \dots, D$  using (3).

**for**  $b = 1, \dots, B$  **do**

3. Draw samples of cluster-level effects  $u_i^{*(b)} = \text{SRSWR}((\hat{u}_1^{sc}, \dots, \hat{u}_D^{sc}), 1)$  for  $i = 1, \dots, D$ .
4. For each  $i = 1, \dots, D$ , sample a donor cluster  $d_i^{(b)} = \text{PPSWR}((1, \dots, D), (n_1, \dots, n_D), 1)$ , then draw samples of unit-level residuals  $e_i^{*(b)} = (e_{i1}^{*(b)}, \dots, e_{in_i}^{*(b)})^\top = \text{SRSWR}(\hat{\mathbf{e}}_{d_i^{(b)}}^s, n_i)$ .
5. Form bootstrap responses as  $\mathbf{y}^{*(b)} = \mathbf{X} \hat{\beta} + \mathbf{Z} \mathbf{u}^{*(b)} + \mathbf{e}^{*(b)}$ , where  $\mathbf{u}^{*(b)} = (u_1^{*(b)}, \dots, u_D^{*(b)})^\top$  and  $\mathbf{e}^{*(b)} = (e_1^{*(b)\top}, \dots, e_D^{*(b)\top})^\top$ .
6. Fit model (1) to  $(\mathbf{y}^{*(b)}, \mathbf{X})$  and obtain  $\hat{\theta}^{*(b)} = (\hat{\beta}^{*(b)\top}, \hat{\sigma}_u^{2*(b)}, \hat{\sigma}_e^{2*(b)})^\top$ .

**Output:** Bootstrap samples  $\{\hat{\theta}^{*(b)} : b = 1, \dots, B\}$ .

---

cluster-level random effect predictors  $\hat{u}_i^{sc}$  and unit-level residuals  $\hat{e}_{ij}^s$  are computed nonparametrically. Consequently, the PREB-1 bootstrap only requires correct specification of the fixed effect structure and can accommodate non-normal random effects and errors. The centering and scaling in equation (3) ensures that  $E^*(u_i^*) = 0$ ,  $E^*(e_{ij}^*) = 0$ ,  $\text{var}^*(u_i^*) = \hat{\sigma}_u^2$ , and  $\text{var}^*(e_{ij}^*) = \hat{\sigma}_e^2$  under all cluster size scenarios, where  $E^*(\cdot)$  and  $\text{var}^*(\cdot)$  denote bootstrap expectation and variance operators conditional on the observed response vector  $\mathbf{y}$ . This property guarantees the consistency of confidence intervals formed by the PREB-1 bootstrap; see Section 3 for the detailed derivations of bootstrap expectations and variances.

The proposed PREB-1 bootstrap differs from the prescaled REB (REB-1) bootstrap of Chambers and Chandra (2013) in two main aspects. First, the REB-1 bootstrap samples the donor cluster  $d_i^{(b)}$  using SRS rather than PPS sampling in Step 4 of Algorithm 1. Second, the REB-1 bootstrap employs a different form of refloating for the cluster-level random effects given by  $\hat{u}_i^{cs} = \hat{\sigma}_u \hat{u}_i^c \{D^{-1} \sum_{i'=1}^D \hat{u}_{i'}^2\}^{-1/2}$  which differs from  $\hat{u}_i^{sc}$  in (3) by using  $\{D^{-1} \sum_{i'=1}^D \hat{u}_{i'}^2\}^{-1/2}$  rather than  $\{D^{-1} \sum_{i'=1}^D (\hat{u}_{i'}^c)^2\}^{-1/2}$  in the denominator. The PREB-1 bootstrap reduces to the REB-1 bootstrap when cluster sizes are balanced. In this setting, the PPS sampling in Step 4 is equivalent

to SRS since the selection probability of cluster  $i$  is  $p_i = (N/D)/N = 1/D$ , and it can be further verified that  $\hat{u}_i^{cs} = \hat{u}_i^{sc}$ . Importantly, these differences lead to improved performance of the PREB-1 bootstrap relative to the REB-1 bootstrap under highly unbalanced cluster sizes, as shown in the simulation study of Section 4.

Two additional variants of the PREB bootstrap are described in supplementary material S1, namely the simple PREB-0 and postscaled PREB-2 bootstraps, which are motivated from the original REB-0 and REB-2 bootstraps of Chambers and Chandra (2013). The PREB-0 bootstrap omits refloating by skipping Step 2 of Algorithm 1, while the PREB-2 bootstrap applies a postscaling adjustment to the PREB-0 bootstrap distributions using mean/ratio correction, noting that these bootstraps do not perform as well as the PREB-1 bootstrap in the simulations of Section 4.

## 2.2 Modified REB-1 Bootstrap

In addition to the PREB bootstraps, we propose a modified REB-1 (MREB-1) bootstrap designed for unbalanced clusters. This modification addresses the limitations of the original REB-1 bootstrap, namely that  $\text{var}^*(u_i^*) \neq \hat{\sigma}_u^2$  and  $\text{var}^*(e_{ij}^*) \neq \hat{\sigma}_e^2$  under the unbalanced case, differently from the PREB-1 bootstrap by selecting donor clusters via SRS rather than PPS sampling and then selecting unit-level residuals from

$$\tilde{e}_{ij}^s = \hat{e}_{ij} \frac{\hat{\sigma}_e}{\sqrt{\sum_{i'=1}^D \sum_{j'=1}^{n_{i'}} D^{-1} n_{i'}^{-1} \hat{e}_{i'j'}^2}}, \quad (4)$$

instead of  $\hat{e}_{ij}^s$ . The full procedure is summarized in Algorithm 2.

Compared to the REB-1 bootstrap, the MREB-1 bootstrap applies an alternative form of refloating for the cluster-level random effects and unit-level residuals. When the cluster sizes are balanced, the MREB-1 bootstrap is equivalent to both PREB-1 and REB-1 bootstraps, owing to the equivalence of PPS sampling and SRS, and  $\hat{u}_i^{sc} = \hat{u}_i^{cs}$  and  $\tilde{e}_{ij}^s = \hat{e}_{ij}^s$ . Like the PREB-1 bootstrap, the MREB-1

---

**Algorithm 2:** Algorithm for the MREB-1 bootstrap.

---

**Input:** ML or REML estimates  $\hat{\theta} = (\hat{\beta}^\top, \hat{\sigma}_u^2, \hat{\sigma}_e^2)^\top$ .

1. Compute marginal residuals  $\mathbf{r}_i = (r_{i1}, \dots, r_{in_i})^\top = \mathbf{y}_i - \mathbf{X}_i \hat{\beta}$  for  $i = 1, \dots, D$ . Obtain cluster-level random effect predictors  $\hat{\mathbf{u}} = (\hat{u}_1, \dots, \hat{u}_D)^\top$  and unit-level residuals  $\hat{\mathbf{e}}_i = (\hat{e}_{i1}, \dots, \hat{e}_{in_i})^\top$  from (2).

2. Reflate these quantities to  $\hat{\mathbf{u}}^{sc} = (\hat{u}_1^{sc}, \dots, \hat{u}_D^{sc})^\top$  using (3) and  $\tilde{\mathbf{e}}_i^s = (\tilde{e}_{i1}^s, \dots, \tilde{e}_{in_i}^s)^\top$  for  $i = 1, \dots, D$  using (4).

**for**  $b = 1, \dots, B$  **do**

3. Draw samples of cluster-level effects  $u_i^{*(b)} = \text{SRSWR}((\hat{u}_1^{sc}, \dots, \hat{u}_D^{sc}), 1)$  for  $i = 1, \dots, D$ .

4. For each  $i = 1, \dots, D$ , sample a donor cluster  $d_i^{(b)} = \text{SRSWR}((1, \dots, D), 1)$ , then draw samples of unit-level residuals  $e_i^{*(b)} = (e_{i1}^{*(b)}, \dots, e_{in_i}^{*(b)})^\top = \text{SRSWR}(\tilde{e}_{d_i^{(b)}}^s, n_i)$ .

5. Form bootstrap responses as  $\mathbf{y}^{*(b)} = \mathbf{X} \hat{\beta} + \mathbf{Z} \mathbf{u}^{*(b)} + \mathbf{e}^{*(b)}$ , where  $\mathbf{u}^{*(b)} = (u_1^{*(b)}, \dots, u_D^{*(b)})^\top$  and  $\mathbf{e}^{*(b)} = (e_1^{*(b)\top}, \dots, e_D^{*(b)\top})^\top$ .

6. Fit model (1) to  $(\mathbf{y}^{*(b)}, \mathbf{X})$  and obtain  $\hat{\theta}^{*(b)} = (\hat{\beta}^{*(b)\top}, \hat{\sigma}_u^{2*(b)}, \hat{\sigma}_e^{2*(b)})^\top$ .

**Output:** Bootstrap samples  $\{\hat{\theta}^{*(b)} : b = 1, \dots, B\}$ .

---

bootstrap only requires a correctly specified fixed effect structure, as the cluster-level random effect predictors  $\hat{u}_i^{sc}$  and unit-level residuals  $\tilde{e}_{ij}^s$  are constructed nonparametrically, and it allows for non-normal  $u_i$  and  $e_{ij}$  in (1). Moreover, the conditions  $E^*(u_i^*) = 0$ ,  $E^*(e_{ij}^*) = 0$ ,  $\text{var}^*(u_i^*) = \hat{\sigma}_u^2$ , and  $\text{var}^*(e_{ij}^*) = \hat{\sigma}_e^2$  are satisfied for the MREB-1 bootstrap under both balanced and unbalanced cases. Therefore, the PREB-1 and MREB-1 bootstraps provide useful alternatives for inference with clustered data, particularly when cluster sizes are highly unbalanced.

### 3 Theoretical Properties of Adjusted REB Bootstraps

This section discusses the theoretical properties of the proposed PREB and MREB-1 bootstraps, as well as the REB bootstraps, under model (1) for both balanced and highly unbalanced cluster sizes. As the ML and REML estimators are asymptotically equivalent when  $p$  is fixed, we focus on the ML estimator  $\hat{\theta}$ . Following Shao et al. (2000) and Carpenter et al. (2003), and under suitable regularity conditions, bootstrap percentile confidence intervals are Fisher consistent if the bootstrap expectations of the ML estimating functions are zero. Under a Gaussian working

likelihood, the ML estimating functions are

$$\frac{\partial l(\boldsymbol{\theta}; \mathbf{y})}{\partial \boldsymbol{\theta}} = \begin{pmatrix} -2\mathbf{X}^\top \boldsymbol{\Sigma}^{-1}(\sigma_u^2, \sigma_e^2)(\mathbf{y} - \mathbf{X}\boldsymbol{\beta}) \\ \frac{1}{2}\text{tr}\left\{\boldsymbol{\Sigma}(\sigma_u^2, \sigma_e^2)\frac{\partial \boldsymbol{\Sigma}^{-1}(\sigma_u^2, \sigma_e^2)}{\partial \sigma_u^2}\right\} - \frac{1}{2}\text{tr}\left\{(\mathbf{y} - \mathbf{X}\boldsymbol{\beta})(\mathbf{y} - \mathbf{X}\boldsymbol{\beta})^\top \frac{\partial \boldsymbol{\Sigma}^{-1}(\sigma_u^2, \sigma_e^2)}{\partial \sigma_u^2}\right\} \\ \frac{1}{2}\text{tr}\left\{\boldsymbol{\Sigma}(\sigma_u^2, \sigma_e^2)\frac{\partial \boldsymbol{\Sigma}^{-1}(\sigma_u^2, \sigma_e^2)}{\partial \sigma_e^2}\right\} - \frac{1}{2}\text{tr}\left\{(\mathbf{y} - \mathbf{X}\boldsymbol{\beta})(\mathbf{y} - \mathbf{X}\boldsymbol{\beta})^\top \frac{\partial \boldsymbol{\Sigma}^{-1}(\sigma_u^2, \sigma_e^2)}{\partial \sigma_e^2}\right\} \end{pmatrix}. \quad (5)$$

It follows that  $E\{\partial l(\boldsymbol{\theta}; \mathbf{y})/\partial \boldsymbol{\theta}\} = \mathbf{0}_{p+2}$  since  $E(\mathbf{y} - \mathbf{X}\boldsymbol{\beta}) = \mathbf{0}_p$  and  $E\{(\mathbf{y} - \mathbf{X}\boldsymbol{\beta})(\mathbf{y} - \mathbf{X}\boldsymbol{\beta})^\top\} - \boldsymbol{\Sigma}(\sigma_u^2, \sigma_e^2) = \mathbf{0}_{N \times N}$ . Thus,  $\hat{\boldsymbol{\theta}}$  is Fisher consistent for  $\boldsymbol{\theta}$ . Analogously, the bootstrap estimator  $\hat{\boldsymbol{\theta}}^*$  is consistent for  $\hat{\boldsymbol{\theta}}$  if  $E^*\{\partial l(\hat{\boldsymbol{\theta}}; \mathbf{y}^*)/\partial \boldsymbol{\theta}\} = \mathbf{0}_{p+2}$ . With  $\mathbf{y}^* = \mathbf{X}\hat{\boldsymbol{\beta}} + \mathbf{u}^* + \mathbf{e}^*$ , this holds provided that  $E^*(u_i^*) = 0$ ,  $E^*(e_{ij}^*) = 0$ ,  $E^*(u_i^{*2}) = \hat{\sigma}_u^2$ ,  $E^*(e_{ij}^{*2}) = \hat{\sigma}_e^2$ , since  $u_i^*$  and  $e_{ij}^*$  are bootstrapped independently. We next show that the PREB-1 and MREB-1 bootstraps satisfy these conditions.

Recall that the PREB-1 bootstrap samples  $u_i^*$  and  $e_{ij}^*$  from  $\hat{u}_i^{sc}$  and  $\hat{e}_{ij}^s$  in (3), and selects donor clusters via PPS sampling. We then obtain

$$\begin{aligned} E^*(u_i^*) &= \sum_{i'=1}^D \frac{1}{D} \hat{u}_{i'}^{sc} = \sum_{i'=1}^D \frac{1}{D} \frac{\hat{\sigma}_u}{\sqrt{\frac{1}{D} \sum_{l=1}^D (\hat{u}_l^c)^2}} \hat{u}_{i'}^c = \frac{\hat{\sigma}_u}{\sqrt{\frac{1}{D} \sum_{l=1}^D (\hat{u}_l^c)^2}} \frac{1}{D} \sum_{i'=1}^D \left( \hat{u}_{i'} - \frac{1}{D} \sum_{l=1}^D \hat{u}_l \right) = 0, \\ E^*(u_i^{*2}) &= \sum_{i'=1}^D \frac{1}{D} (\hat{u}_{i'}^{sc})^2 = \frac{\hat{\sigma}_u^2}{\frac{1}{D} \sum_{l=1}^D (\hat{u}_l^c)^2} \frac{1}{D} \sum_{i'=1}^D (\hat{u}_{i'}^c)^2 = \hat{\sigma}_u^2, \\ E^*(e_{ij}^*) &= \sum_{i'=1}^D \sum_{j'=1}^{n_{i'}} \frac{n_{i'}}{N} \frac{1}{n_{i'}} \hat{e}_{i'j'}^s = \sum_{i'=1}^D \sum_{j'=1}^{n_{i'}} \frac{n_{i'}}{N} \frac{1}{n_{i'}} \frac{\hat{\sigma}_e}{\sqrt{\frac{1}{N} \sum_{l=1}^D \sum_{m=1}^{n_l} \hat{e}_{lm}^2}} \hat{e}_{i'j'} \\ &= \frac{\hat{\sigma}_e}{\sqrt{\frac{1}{N} \sum_{l=1}^D \sum_{m=1}^{n_l} \hat{e}_{lm}^2}} \sum_{i'=1}^D \frac{n_{i'}}{N} \frac{1}{n_{i'}} \sum_{j'=1}^{n_{i'}} \left( r_{i'j'} - \frac{1}{n_i'} \sum_{m=1}^{n_i'} r_{i'm} \right) = 0, \text{ and} \\ E^*(e_{ij}^{*2}) &= \sum_{i'=1}^D \sum_{j'=1}^{n_{i'}} \frac{n_{i'}}{N} \frac{1}{n_{i'}} (\hat{e}_{ij}^s)^2 = \frac{\hat{\sigma}_e^2}{\frac{1}{N} \sum_{l=1}^D \sum_{m=1}^{n_l} \hat{e}_{lm}^2} \sum_{i'=1}^D \sum_{j'=1}^{n_{i'}} \frac{n_{i'}}{N} \frac{1}{n_{i'}} \hat{e}_{i'j'}^2 \\ &= \frac{\hat{\sigma}_e^2}{\frac{1}{N} \sum_{l=1}^D \sum_{m=1}^{n_l} \hat{e}_{lm}^2} \frac{1}{N} \sum_{i'=1}^D \sum_{j'=1}^{n_{i'}} \hat{e}_{i'j'}^2 = \hat{\sigma}_e^2. \end{aligned}$$

As noted in Section 2.2, the MREB-1 bootstrap only differs from the PREB-1 bootstrap in the bootstrapping of  $e_{ij}^*$  but not  $u_i^*$ . Therefore, the same derivations for  $u_i^*$  apply, giving  $E^*(u_i^*) = 0$

and  $E^*(u_i^{*2}) = \hat{\sigma}_u^2$ . For  $e_{ij}^*$  under the MREB-1 bootstrap, we obtain

$$\begin{aligned} E^*(e_{ij}^*) &= \sum_{i'=1}^D \sum_{j'=1}^{n_{i'}} \frac{1}{D} \frac{1}{n_{i'}} \tilde{e}_{i'j'}^s = \sum_{i'=1}^D \sum_{j'=1}^{n_{i'}} \frac{1}{D} \frac{1}{n_{i'}} \frac{\hat{\sigma}_e}{\sqrt{\sum_{l=1}^D \sum_{m=1}^{n_l} \frac{1}{D} \frac{1}{n_l} \hat{e}_{lm}^2}} \hat{e}_{i'j'} \\ &= \frac{\hat{\sigma}_e}{\sqrt{\sum_{l=1}^D \sum_{m=1}^{n_l} \frac{1}{D} \frac{1}{n_l} \hat{e}_{lm}^2}} \sum_{i'=1}^D \frac{1}{D} \frac{1}{n_{i'}} \sum_{j'=1}^{n_{i'}} \left( r_{i'j'} - \frac{1}{n_{i'}} \sum_{m=1}^{n_{i'}} r_{i'm} \right) = 0, \text{ and} \\ E^*(e_{ij}^{*2}) &= \sum_{i'=1}^D \sum_{j'=1}^{n_{i'}} \frac{1}{D} \frac{1}{n_{i'}} \left( \tilde{e}_{ij}^s \right)^2 = \frac{\hat{\sigma}_e^2}{\sum_{l=1}^D \sum_{m=1}^{n_l} \frac{1}{D} \frac{1}{n_l} \hat{e}_{lm}^2} \sum_{i'=1}^D \sum_{j'=1}^{n_{i'}} \frac{1}{D} \frac{1}{n_{i'}} \hat{e}_{i'j'}^2 = \hat{\sigma}_e^2. \end{aligned}$$

The derivations for the PREB-1 and MREB-1 bootstraps remain valid for general cluster sizes  $n_i$ , confirming that both bootstraps satisfy the required consistency conditions under balanced and highly unbalanced scenarios.

Similar derivations for the REB bootstraps and the PREB-0 and PREB-2 variants are given in supplementary material S2, showing that none of these satisfy the consistency requirements under general cluster size scenarios. In particular, the REB-1 bootstrap, which samples  $u_i^*$  and  $e_{ij}^*$  from  $\hat{u}_i^{cs}$  and  $\hat{e}_{ij}^s$  and uses SRS for donor cluster selection, fails to satisfy  $E^*(u_i^{*2}) = \hat{\sigma}_u^2$  and  $E^*(e_{ij}^{*2}) = \hat{\sigma}_e^2$  when cluster sizes are unbalanced. This highlights the need to sample  $u_i^*$  from  $\hat{u}_i^{sc}$  rather than  $\hat{u}_i^{cs}$  and to pair the donor cluster sampling scheme with the correct residual scaling, e.g., PPS sampling with  $\hat{e}_{ij}^s$  in the PREB-1 bootstrap or SRS with  $\tilde{e}_{ij}^s$  in the MREB-1 bootstrap, to ensure consistency. The PREB-0 and REB-0 bootstraps also fail to satisfy the second moment conditions under both balanced and unbalanced cases, and additionally violate  $E^*(u_i^*) = 0$  in the latter case. Although the PREB-2 and REB-2 bootstraps center the bootstrap distributions at  $\hat{\theta}$ , their bootstrap variance estimators remain invalid because they inherit the inconsistency of the underlying PREB-0 or REB-0 bootstraps.

## 4 Simulation Study

We conducted a simulation study to evaluate the finite sample inferential performance of the proposed bootstraps for clustered data, where the true data generating process follows (1). We set the dimension of the covariate vectors  $\mathbf{x}_{ij} = (1, x_{ij,1})^\top$  to be  $p = 2$ , with  $x_{ij,1} \stackrel{i.i.d.}{\sim} U(0, 1)$  uniformly distributed, and the true fixed effects as  $\beta = (\beta_0, \beta_1)^\top = (1, 2)^\top$ . We considered  $D = 100$  clusters under two cluster size scenarios i.e.,  $n_i = 7$  for  $i = 1, \dots, D$  and  $n_i$  that were highly unbalanced with cluster sizes ranging from 1 to 42. Figure 1 presents the histogram of cluster sizes in the unbalanced scenario, which is qualitatively similar to that of the real data (Figure 2 in Section 5) with the main difference being  $D = 488$  in the real data. The total number of observations was  $N = 700$  for the balanced scenario and  $N = 752$  for the unbalanced scenario. We considered two different settings to simulate the cluster-level random effects  $u_i$  and unit-level error terms  $e_{ij}$ . In set I,  $u_i \stackrel{i.i.d.}{\sim} N(0, \sigma_u^2)$  and  $e_{ij} \stackrel{i.i.d.}{\sim} N(0, \sigma_e^2)$  were normally distributed with  $\sigma_u^2 = 0.04$  and  $\sigma_e^2 = 0.16$ . In set II,  $u_i \stackrel{i.i.d.}{\sim} \sigma_u \{(\chi_1^2 - 1)/\sqrt{2}\}$  and  $e_{ij} \stackrel{i.i.d.}{\sim} \sigma_e \{(\chi_1^2 - 1)/\sqrt{2}\}$ , giving  $\chi^2$  distributions with mean zero and the same variances. Sets I and II were also considered in the simulation study of [Chambers and Chandra \(2013\)](#) who focused on balanced clusters. A total of 500 datasets was simulated for each of the four combinations of cluster size scenarios (balanced/unbalanced) and settings (I/II).

We applied our proposed PREB bootstraps (PREB-0/1/2) and the MREB-1 bootstrap, alongside the REB bootstraps (REB-0/1/2) of [Chambers and Chandra \(2013\)](#) to each simulated dataset. For comparison, we also implemented commonly used clustered data bootstrap methods, including: (i) the parametric bootstrap, generating  $u_i^* \sim N(0, \hat{\sigma}_u^2)$  and  $e_{ij}^* \sim N(0, \hat{\sigma}_e^2)$ , (ii) the cluster bootstrap ([Davison and Hinkley, 1997](#); [McCullagh, 2000](#)), resampling entire clusters, i.e.,  $\mathbf{y}^* = (\mathbf{y}_{h_1}^\top, \dots, \mathbf{y}_{h_D}^\top)^\top$  and  $\mathbf{X}^* = (\mathbf{X}_{h_1}^\top, \dots, \mathbf{X}_{h_D}^\top)^\top$  with  $h_i = \text{SRSWR}((1, \dots, D), 1)$ , (iii) the generalized cluster bootstrap, resampling cluster weights  $w_i^* \sim \text{Exp}(1)$  from the standard exponential distribution and maximizing the weighted log-likelihood  $\sum_{i=1}^D w_i^* l_i(\boldsymbol{\theta}; \mathbf{y}_i, \mathbf{X}_i)$

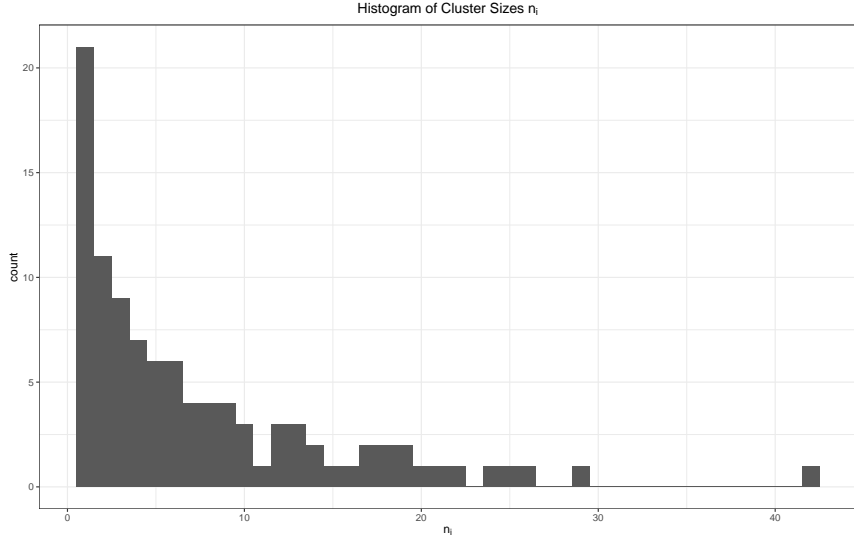


Figure 1: Histogram of cluster sizes  $n_i$  for  $i = 1, \dots, 100$  clusters in the simulated data.

(Field et al., 2010; O’Shaughnessy and Welsh, 2018), (iv) the CGR semiparametric bootstrap (Carpenter et al., 2003), resampling  $u_i^* = \text{SRSWR}(\hat{\sigma}_u(D^{-1}\sum_{i=1}^D \tilde{u}_i^2)^{-1/2}(\tilde{u}_1, \dots, \tilde{u}_D), 1)$  and  $e_{ij}^* = \text{SRSWR}(\hat{\sigma}_e(N^{-1}\sum_{i=1}^D \sum_{j=1}^{n_i} \hat{\epsilon}_{ij}^2)^{-1/2}(\hat{\epsilon}_{11}, \dots, \hat{\epsilon}_{Dn_D}), 1)$  with  $\tilde{u}_i$ ’s denoting the EBLUPs of the cluster-level random effects and  $\hat{\epsilon}_{ij} = y_{ij} - \mathbf{x}_{ij}^\top \hat{\beta} - \tilde{u}_i$ , and (v) modifications of the REB bootstraps (REBnc-0/1) without random donor cluster sampling (Reluga et al., 2024). For all methods,  $B = 500$  bootstrap replicates were used. We assessed performance based on the empirical coverage rates of 95% bootstrap percentile confidence intervals for  $\theta = (\beta^\top, \sigma_u^2, \sigma_e^2) = (1, 2, 0.04, 0.16)$  and the signal-to-noise ratio  $\lambda = \sigma_u^2/\sigma_e^2 = 0.25$ , computed over the 500 simulated datasets.

Tables 1 shows that among the four proposed bootstrap methods (PREB-0/1/2 and MREB-1), the PREB-1 and MREB-1 bootstraps consistently achieve coverage rates closest to the nominal 95% level for all parameters, despite some overcoverage for  $\sigma_e^2$ . This aligns with the theoretical results in Section 3, as both methods satisfy the consistency requirements under the balanced and unbalanced scenarios. In contrast, the PREB-0 and PREB-2 bootstraps provide good coverage for  $\beta_0$  and  $\beta_1$  but tend to exhibit undercoverage for the variance components and the signal-to-noise ratio, particularly under unbalanced clusters. The undercoverage is less severe for the PREB-2 bootstrap due to the centering adjustment.

Table 1: Empirical coverage rate of 95% bootstrap percentile confidence intervals using various bootstrap methods for sets I (left panel) and II (right panel) under balanced (top panel) and highly unbalanced (bottom panel) cluster sizes.

	Set I (Balanced)					Set II (Balanced)				
	$\beta_0$	$\beta_1$	$\sigma_u^2$	$\sigma_e^2$	$\lambda$	$\beta_0$	$\beta_1$	$\sigma_u^2$	$\sigma_e^2$	$\lambda$
PREB-0	0.954	0.926	0.484	0.464	0.246	0.956	0.926	0.822	0.828	0.708
PREB-1	0.948	0.952	0.944	0.990	0.942	0.946	0.948	0.894	0.976	0.926
PREB-2	0.952	0.926	0.880	0.996	0.880	0.956	0.930	0.820	0.978	0.846
MREB-1	0.944	0.950	0.944	0.994	0.956	0.944	0.938	0.892	0.972	0.920
REB-0	0.958	0.936	0.484	0.438	0.242	0.950	0.922	0.824	0.828	0.708
REB-1	0.944	0.948	0.944	0.996	0.946	0.946	0.938	0.898	0.974	0.924
REB-2	0.954	0.938	0.876	0.994	0.884	0.952	0.926	0.826	0.980	0.846
Parametric Bootstrap	0.946	0.952	0.938	0.958	0.936	0.948	0.938	0.742	0.604	0.732
Cluster Bootstrap	0.954	0.956	0.926	0.954	0.930	0.950	0.938	0.866	0.912	0.910
Generalized Cluster Bootstrap	0.946	0.946	0.904	0.948	0.916	0.948	0.934	0.862	0.898	0.892
CGR Bootstrap	0.946	0.950	0.934	0.960	0.938	0.954	0.946	0.846	0.882	0.854
REBnc-0	0.950	0.932	0.486	0.154	0.228	0.958	0.932	0.822	0.588	0.638
REBnc-1	0.938	0.948	0.938	0.954	0.940	0.954	0.944	0.896	0.852	0.914
Set I (Unbalanced)						Set II (Unbalanced)				
	$\beta_0$	$\beta_1$	$\sigma_u^2$	$\sigma_e^2$	$\lambda$	$\beta_0$	$\beta_1$	$\sigma_u^2$	$\sigma_e^2$	$\lambda$
PREB-0	0.972	0.938	0.014	0.680	0.006	0.948	0.928	0.392	0.908	0.384
PREB-1	0.950	0.950	0.954	1.000	0.958	0.926	0.934	0.886	0.990	0.938
PREB-2	0.988	0.938	0.884	1.000	0.900	0.966	0.926	0.798	0.984	0.852
MREB-1	0.946	0.956	0.968	1.000	0.986	0.926	0.932	0.922	0.998	0.972
REB-0	0.956	0.896	0.014	0.012	0.000	0.924	0.876	0.340	0.468	0.128
REB-1	0.916	0.910	0.944	0.252	0.916	0.886	0.892	0.890	0.768	0.966
REB-2	0.972	0.896	0.860	1.000	0.924	0.948	0.874	0.784	1.000	0.884
Parametric Bootstrap	0.956	0.954	0.910	0.936	0.912	0.942	0.936	0.708	0.584	0.684
Cluster Bootstrap	0.952	0.944	0.910	0.924	0.916	0.920	0.926	0.856	0.900	0.898
Generalized Cluster Bootstrap	0.938	0.948	0.898	0.918	0.910	0.924	0.920	0.848	0.894	0.864
CGR Bootstrap	0.946	0.950	0.946	0.928	0.936	0.924	0.924	0.844	0.886	0.870
REBnc-0	0.970	0.938	0.076	0.358	0.040	0.940	0.920	0.584	0.720	0.496
REBnc-1	0.950	0.956	0.864	0.924	0.870	0.920	0.938	0.762	0.874	0.798

Among the three variants of REB bootstraps, the REB-1 bootstrap performs best under the balanced scenario, consistent with the findings of [Chambers and Chandra \(2013\)](#). The PREB and MREB-1 bootstraps have comparable performance to their REB counterparts under balanced clusters, reflecting their equivalence in this scenario. Under highly unbalanced clusters, all REB bootstraps suffer from undercoverage for  $\beta_1$ , while the PREB and MREB-1 bootstraps maintain coverage near 95%. For variance components and  $\lambda$ , our proposed PREB-1 and MREB-1 bootstraps outperform all REB bootstraps, including the REB-1 bootstrap that undercovers  $\sigma_e^2$  and  $\lambda$  under set I (unbalanced) and  $\sigma_u^2$  and  $\sigma_e^2$  under set II (unbalanced).

Compared to other common bootstrap methods (parametric, cluster, generalized cluster, CGR and

REBnc-0/1), the PREB-1 and MREB-1 bootstraps generally outperform these alternatives in terms of coverage for variance components and  $\lambda$  under set I (unbalanced), except for the CGR bootstrap that performs equally well. When random effects and error terms are chi-squared distributed (set II), coverage for  $\sigma_u^2$  and  $\lambda$  using the PREB-1 and MREB-1 bootstraps is reduced. Notably, the alternative methods show even worse coverage for not only  $\sigma_u^2$  and  $\lambda$  but also  $\sigma_e^2$  in this chi-squared setting, particularly those that rely on normality assumptions such as the parametric bootstrap and, interestingly, the CGR bootstrap.

Supplementary simulations with unit-level errors  $e_{ij}$  generated from first-order autoregressive (AR-1) models to induce correlated residuals, under both balanced and unbalanced clusters, are reported in Table S1 of supplementary material S3. Overall, the relative performance of bootstrap methods is qualitatively similar to Table 1, though undercoverage for  $\sigma_u^2$ ,  $\sigma_e^2$  and  $\lambda$  is greater than set II when  $e_{ij}$  are correlated. The PREB-1 and MREB-1 bootstraps still outperform other approaches, particularly in the unbalanced case. We also include autoregressive variants of PREB bootstraps which fit model (1) with an AR-1 error covariance and generate bootstrap samples  $e_{ij}^*$  preserving the AR-1 dependence in the same supplementary simulations. Results indicate that the autoregressive variant of the PREB-1 bootstrap achieves close to 95% coverage for  $\sigma_u^2$ ,  $\sigma_e^2$  and  $\lambda$ . Motivated by the numerical study of Chambers and Chandra (2013), additional simulations for larger balanced clusters ( $n_i = 20$ ) under sets I, II, and AR-1 error settings are reported in Table S2 of supplementary material S3. Results for sets I and II are consistent with  $n_i = 7$ , while for AR-1 errors, larger cluster sizes improve coverage for  $\sigma_u^2$ ,  $\sigma_e^2$ , and  $\lambda$  across all methods, with the autoregressive variant of the PREB-1 bootstrap continuing to perform best.

## 5 Application to Oman Rainfall Enhancement Trial Dataset

The Oman rainfall enhancement trial data studied in Chambers et al. (2022a,b) were collected during a randomized trial of ground-based ionization technology in the Hajar Mountains, Oman

between 2013 to 2018. The trial began with two ionizers and 120 rain gauges in 2013, expanding to ten ionizers (denoted as H1 - H10) and 201 rain gauges in 2018; see [Chambers et al. \(2022a\)](#) for more details of the trial. Its objective was to investigate whether exposure to an operating ionizer increases the amount of rainfall measured by the rain gauges downwind of the ionizer.

The dataset comprises  $N = 4168$  gauge-day observations with positive rainfall recorded downwind of deployed ionizers. It also includes daily meteorological variables and gauge-specific topographical information. Let  $i$  index days and  $j$  index gauges. Following [Chambers et al. \(2022a,b\)](#), we model log-rainfall using the random intercept model

$$y_{ij} = \mathbf{x}_{ij, \text{non-ionizer}}^\top \boldsymbol{\beta}_{\text{non-ionizer}} + \mathbf{x}_{ij, \text{ionizer}}^\top \boldsymbol{\beta}_{\text{ionizer}} + u_i + e_{ij}, \quad (6)$$

for  $j = 1, \dots, n_i$  and  $i = 1, \dots, D$ , where  $y_{ij}$  denotes the log-transformed positive rainfall at downwind gauge  $j$  on day  $i$ ,  $\mathbf{x}_{ij, \text{non-ionizer}}$  is a covariate vector containing an intercept, elevation and expected natural rainfall, and  $\mathbf{x}_{ij, \text{ionizer}}$  consists of ten binary target indicators for ionizers H1–H10, e.g., the H1 indicator equals one only if the gauge is downwind of H1 on day  $i$  and H1 was turned on, plus interactions of elevation with H1 and H2 indicators. The expected natural rainfall covariate in  $\mathbf{x}_{ij, \text{non-ionizer}}$  represents the natural downwind rainfall that would have been observed if there were no ionizers; these were obtained as fitted values from a preliminary random intercept model fitted to the log-rainfall of upwind gauges using meteorological covariates; see Table 3 of [Chambers et al. \(2022a\)](#). The random intercepts  $u_i$  capture day-to-day variation in rainfall, and are assumed i.i.d. with mean 0 and variance  $\sigma_u^2$ , while  $e_{ij}$  are i.i.d. with mean 0 and variance  $\sigma_e^2$ . Parameter estimates are reported in Table S3 of supplementary material S4.

In this dataset, the total number of trial days (clusters) with at least one downwind gauge recording positive rainfall was  $D = 488$ , with cluster sizes  $n_i$  (number of downwind gauges recording positive rainfall on day  $i$ ) ranging from 1 to 58. Figure 2 provides a histogram of  $n_i$ , illustrating the highly unbalanced cluster sizes due to variability in precipitation.

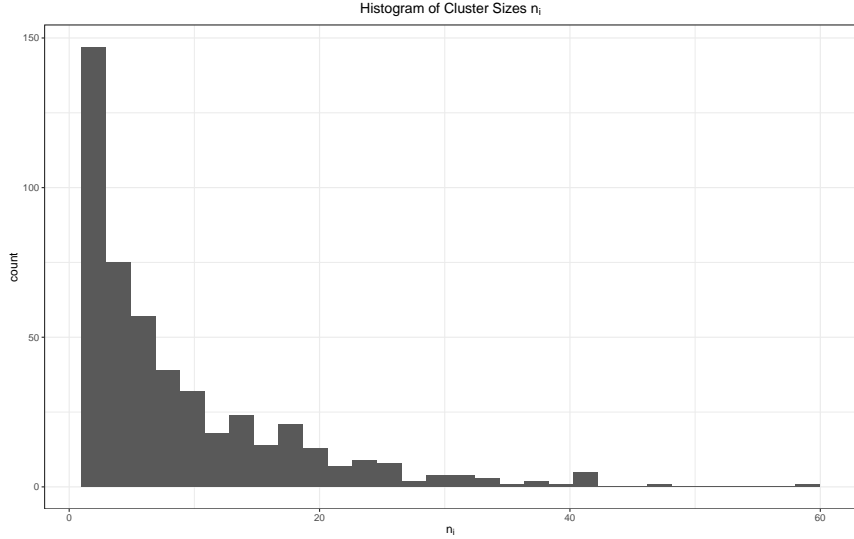


Figure 2: Histogram of cluster sizes  $n_i$  for  $i = 1, \dots, 488$  days in the Oman rainfall enhancement trial data.

To study ionization effectiveness, [Chambers et al. \(2022a\)](#) defined the ‘attribution’

$$\gamma = \frac{\sum_{i=1}^D \sum_{j=1}^{n_i} \{ \exp(y_{ij}) - \exp(y_{ij}) \exp(-\mathbf{x}_{ij,ionizer}^\top \boldsymbol{\beta}_{ionizer}) \}}{\sum_{i=1}^D \sum_{j=1}^{n_i} \exp(y_{ij}) \exp(-\mathbf{x}_{ij,ionizer}^\top \boldsymbol{\beta}_{ionizer})} \times 100\%,$$

where the denominator represents total downwind rainfall without ionizer effects, and the numerator represents the change in rainfall attributable to ionization. The point estimate

$$\hat{\gamma} = \frac{\sum_{i=1}^D \sum_{j=1}^{n_i} \{ \exp(y_{ij}) - \exp(y_{ij}) \kappa^{-1}(\mathbf{y}, \hat{\boldsymbol{\theta}}) \exp(-\mathbf{x}_{ij,ionizer}^\top \hat{\boldsymbol{\beta}}_{ionizer}) \}}{\sum_{i=1}^D \sum_{j=1}^{n_i} \exp(y_{ij}) \kappa^{-1}(\mathbf{y}, \hat{\boldsymbol{\theta}}) \exp(-\mathbf{x}_{ij,ionizer}^\top \hat{\boldsymbol{\beta}}_{ionizer})} \times 100\% = 12.52\%, \quad (7)$$

uses parameter estimates  $\hat{\boldsymbol{\theta}} = (\hat{\boldsymbol{\beta}}_{non-ionizer}^\top, \hat{\boldsymbol{\beta}}_{ionizer}^\top, \hat{\sigma}_u^2, \hat{\sigma}_e^2)^\top$  from (6) and a smearing-type correction  $\kappa(\mathbf{y}, \hat{\boldsymbol{\theta}})$  ([Duan, 1983](#)), which is a function of  $\mathbf{y}$  and  $\hat{\boldsymbol{\theta}}$ , to correct for transformation bias; see [Chambers et al. \(2022a\)](#) for details. Inference for  $\gamma$  was obtained using its REB-1 bootstrap distribution  $\{\hat{\gamma}^{*(b)} : b = 1, \dots, B\}$ , where each  $\hat{\gamma}^*$  was computed by replacing  $y_{ij}$ ,  $\mathbf{y}$ ,  $\hat{\boldsymbol{\beta}}_{ionizer}$  and  $\hat{\boldsymbol{\theta}}$  in (7) with the corresponding bootstrap samples  $y_{ij}^*$ ,  $\mathbf{y}^*$ ,  $\hat{\boldsymbol{\beta}}_{ionizer}^*$  and  $\hat{\boldsymbol{\theta}}^*$ . From a causal perspective, [Chambers et al. \(2022b\)](#) classified gauge-days with nonzero (zero)  $x_{ij,ionizer}$  as treated (control) observations and focused on the sample average treatment effect (SATE)

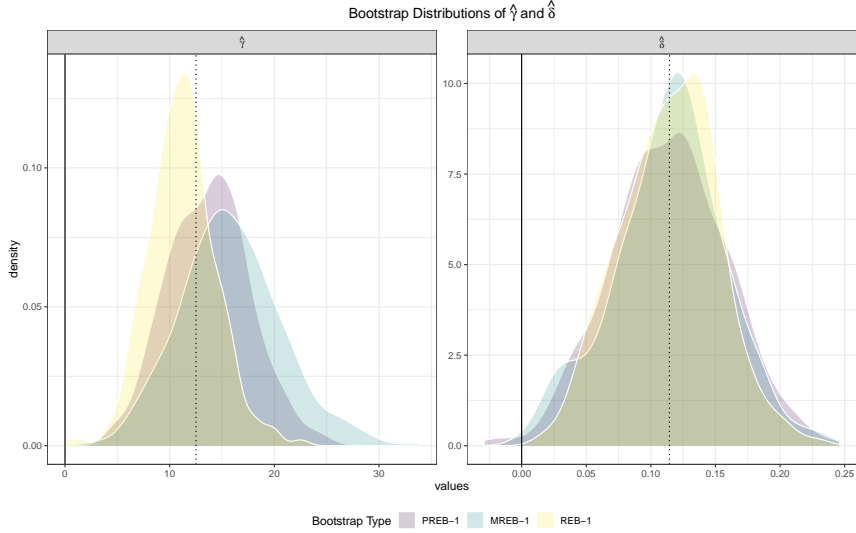


Figure 3: Bootstrap distributions of  $\hat{\gamma}$  (left) and  $\hat{\delta}$  (right) using PREB-1 (purple), MREB-1 (green) and REB-1 (yellow), where vertical dotted lines represent point estimates and vertical solid lines represent zero.

Table 2: Bootstrap p-values for  $\gamma$  and  $\delta$  using PREB-1, MREB-1 and REB-1 bootstraps.

	PREB-1	MREB-1	REB-1		PREB-1	MREB-1	REB-1
$\gamma$	0.000	0.000	0.000	$\delta$	0.008	0.002	0.000

$\delta = N^{-1} \sum_{i=1}^D \sum_{j=1}^{n_i} E(y_{ij,1} | \mathbf{x}_{ij,non-ionizer}) - E(y_{ij,0} | \mathbf{x}_{ij,non-ionizer})$ , where  $y_{ij,1}$  and  $y_{ij,0}$  denote potential responses under treatment and control, respectively. The model-based estimate for the SATE is  $\hat{\delta} = \{\sum_{i=1}^D \sum_{j=1}^{n_i} I_{ij} (\mathbf{x}_{ij,ionizer}^\top \hat{\beta}_{ionizer})\} / (\sum_{i=1}^D \sum_{j=1}^{n_i} I_{ij}) = 0.114$ , where  $I_{ij} = 1$  for treated observations and 0 otherwise. The REB-1 distribution  $\{\hat{\delta}^{*(b)} : b = 1, \dots, B\}$  was also used for inference on  $\delta$ , with  $\hat{\delta}^*$  obtained by replacing  $\hat{\beta}_{ionizer}$  in  $\hat{\delta}$  with the bootstrap samples  $\hat{\beta}_{ionizer}^*$ . Since the REB-1 bootstrap has been shown in the simulation study to underperform under highly unbalanced cluster sizes like those in this dataset, we use the PREB-1 and MREB-1 bootstraps, which are more reliable under such scenarios.

Figure 3 presents the bootstrap distributions of  $\hat{\gamma}$  and  $\hat{\delta}$  under the PREB-1, MREB-1 and REB-1 bootstraps (each with  $B = 500$  replicates), while Table 2 provides the corresponding bootstrap p-values, defined as the proportion of bootstrap samples less than or equal to zero. All three methods indicate a positive and significant effect of ionization on downwind rainfall at the 5% significance

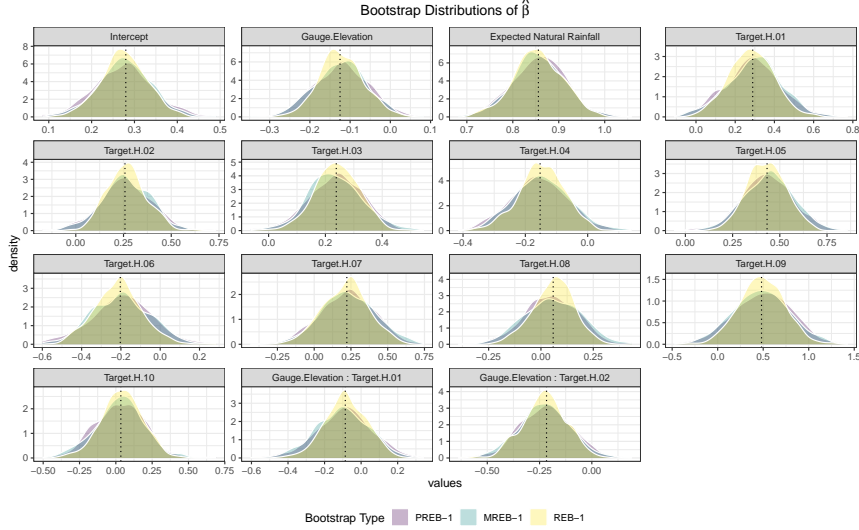


Figure 4: Bootstrap distributions of elements of  $\hat{\beta}$  using PREB-1 (purple), MREB-1 (green) and REB-1 (yellow), where vertical dotted lines represent point estimates.

level. However, there are some differences between the REB-1 distributions and the proposed PREB-1 and MREB-1 distributions: the REB-1 distribution for  $\gamma$  is shifted to the left, and its distributions for both  $\gamma$  and  $\delta$  are slightly more concentrated, resulting in more significant p-values. As such, the more conservative PREB-1 and MREB-1 results may be preferable in the presence of highly unbalanced cluster sizes. This is further supported by the bootstrap distributions of the fixed effects and variance components in Figures 4 – 5. Specifically, the REB-1 bootstrap distributions for all fixed effects are always the narrowest, aligning with the undercoverage observed under unbalanced clusters in Section 4. Moreover, the REB-1 bootstrap distributions for  $\sigma_e^2$  and  $\lambda$  (signal to noise ratio) are not centered on the point estimates, reflecting poor coverage in the simulation study. In contrast, the PREB-1 and MREB-1 bootstrap distributions are well centered around the point estimates. These results substantiate the use of the PREB-1 and MREB-1 bootstraps, which exhibited improved coverage performance. This application highlights the advantages of our proposed bootstraps for conducting inference, not only on the random intercept model parameters, but also on complex functions of these parameters, including the attribution  $\gamma$  and SATE  $\delta$ .

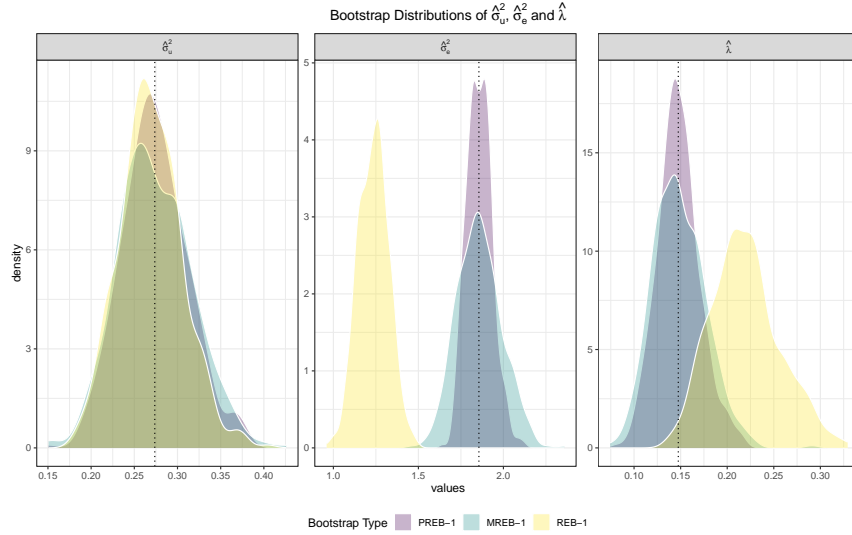


Figure 5: Bootstrap distributions of  $\hat{\sigma}_u^2$  (left),  $\hat{\sigma}_e^2$  (middle) and  $\hat{\lambda}$  (right) using PREB-1 (purple), MREB-1 (green) and REB-1 (yellow), where vertical dotted lines represent point estimates.

## 6 Conclusion

We develop the PREB-1 and MREB-1 bootstraps for clustered data with general cluster sizes. These methods extend the REB bootstraps, originally designed for balanced cluster sizes, allowing general distributions of random effects and error terms in linear mixed models. We demonstrate the Fisher consistency of our proposed bootstraps under both balanced and unbalanced cluster sizes, and show that the REB bootstraps are consistent only for the balanced case. A key feature of our approach is the use of proper centering and scaling of the random effect and residual predictors prior to resampling, paired with an appropriate cluster resampling scheme. Simulation studies show the strong finite sample inferential performance of the PREB-1 and MREB-1 bootstraps, which demonstrate superior performance compared to the REB bootstraps when cluster sizes are highly unbalanced, and outperform other commonly used bootstraps for clustered data such as the parametric bootstrap and the CGR bootstrap when the underlying random effects and error terms are chi-squared distributed. We apply these methods and the REB bootstraps to the Oman rainfall enhancement trial data to conduct inference on both the fixed effects and variance components, as well as more complicated functions of these parameters. While all methods indicate a statistically

significant positive effect of the ionization technology on rainfall, our proposed bootstraps yielded larger, and arguably more reasonable, estimates of variability, given that the REB bootstrap distributions of the variance components are not centered at the point estimates.

A natural extension of the PREB-1 and MREB-1 bootstraps is to accommodate non-continuous responses by replacing the linear mixed model (1) with a generalized linear mixed model (Breslow and Clayton, 1993), where the conditional mean of the response is modelled as a linear function of the covariates and random effects through a suitable link function. This would broaden applicability to fields involving discrete responses in a clustered data setting, such as ecology where  $y_{ij}$  are the presence-absence records or counts of species  $j$  in sampling site  $i$ . Another direction is to extend our bootstraps to perform inference on linear combinations of fixed effects and random effects  $\mathbf{l}_i^\top \boldsymbol{\beta} + u_i$ , which are also known as cluster-level mixed effects parameters; see the recent work of Reluga et al. (2024) who considered bootstrap inference for such parameters in random slope models. Finally, it would be useful to investigate alternative confidence interval constructions based on the PREB-1 and MREB-1 bootstrap distributions, e.g., basic bootstrap confidence interval (Davison and Hinkley, 1997), bootstrap- $t$  confidence interval (Efron, 1981), and bias-corrected and accelerated confidence interval (Efron, 1987), and compare their performance to our bootstrap percentile confidence intervals across different cluster size scenarios.

## SUPPLEMENTARY MATERIAL

**Supplementary Results and Details:** Descriptions of the PREB-0 and PREB-2 bootstraps, detailed derivation of theoretical properties of the proposed and REB bootstraps, and additional results for simulations and the real data application. (.pdf file).

## References

Bates, D., Mächler, M., Bolker, B., and Walker, S. (2015). Fitting linear mixed-effects models using lme4. *Journal of Statistical Software*, 67:1–48.

Breslow, N. E. and Clayton, D. G. (1993). Approximate inference in generalized linear mixed models. *Journal of the American Statistical Association*, 88:9–25.

Butar, F. B. and Lahiri, P. (2003). On measures of uncertainty of empirical Bayes small-area estimators. *Journal of Statistical Planning and Inference*, 112:63–76. Special issue II: Model Selection, Model Diagnostics, Empirical Bayes and Hierarchical Bayes.

Bühlmann, P. (1997). Sieve bootstrap for time series. *Bernoulli*, 3:123–148.

Carpenter, J. R., Goldstein, H., and Rasbash, J. (2003). A novel bootstrap procedure for assessing the relationship between class size and achievement. *Journal of the Royal Statistical Society: Series C (Applied Statistics)*, 52:431–443.

Castillo-Páez, S., Fernández-Casal, R., and García-Soidán, P. (2019). A nonparametric bootstrap method for spatial data. *Computational Statistics & Data Analysis*, 137:1–15.

Chambers, R., Beare, S., Peak, S., and Al-Kalbani, M. (2022a). Nudging a pseudo-science towards a science—the role of statistics in a rainfall enhancement trial in Oman. *International Statistical Review*, 90:346–373.

Chambers, R. and Chandra, H. (2013). A random effect block bootstrap for clustered data. *Journal of Computational and Graphical Statistics*, 22:452–470.

Chambers, R., Ranjbar, S., Salvati, N., and Pacini, B. (2022b). Weighting, informativeness and causal inference, with an application to rainfall enhancement. *Journal of the Royal Statistical Society Series A: Statistics in Society*, 185:1584–1612.

Chatterjee, S. and Bose, A. (2005). Generalized bootstrap for estimating equations. *The Annals of Statistics*, 33:414–436.

Davison, A. and Hinkley, D. (1997). *Bootstrap Methods and Their Application*. Bootstrap Methods and Their Application. Cambridge University Press.

Duan, N. (1983). Smearing estimate: A nonparametric retransformation method. *Journal of the American Statistical Association*, 78:605–610.

Efron, B. (1979). Bootstrap methods: Another look at the jackknife. *The Annals of Statistics*, 7:1–26.

Efron, B. (1981). Nonparametric standard errors and confidence intervals. *Canadian Journal of Statistics*, 9:139–158.

Efron, B. (1987). Better bootstrap confidence intervals. *Journal of the American Statistical Association*, 82:171–185.

Efron, B. and Tibshirani, R. (1994). *An Introduction to the Bootstrap*. Chapman & Hall/CRC Monographs on Statistics & Applied Probability. Taylor & Francis.

Field, C. A., Pang, Z., and Welsh, A. H. (2010). Bootstrapping robust estimates for clustered data. *Journal of the American Statistical Association*, 105:1606–1616.

Friedrich, M. and Lin, Y. (2024). Sieve bootstrap inference for linear time-varying coefficient models. *Journal of Econometrics*, 239:105345. Climate Econometrics.

Hall, P. (1992). *The Bootstrap and Edgeworth Expansion*. Springer Series in Statistics. Springer New York.

Harville, D. A. (1977). Maximum likelihood approaches to variance component estimation and to related problems. *Journal of the American Statistical Association*, 72:320–338.

Kubokawa, T. and Nagashima, B. (2012). Parametric bootstrap methods for bias correction in

linear mixed models. *Journal of Multivariate Analysis*, 106:1–16.

Künsch, H. R. (1989). The jackknife and the bootstrap for general stationary observations. *The*

*Annals of Statistics*, 17:1217–1241.

Lahiri, S. N. and Zhu, J. (2006). Resampling methods for spatial regression models under a class

of stochastic designs. *The Annals of Statistics*, 34(4):1774–1813.

McCullagh, P. (2000). Resampling and exchangeable arrays. *Bernoulli*, 6:285–301.

O’Shaughnessy, P. and Welsh, A. (2018). Bootstrapping longitudinal data with multiple levels of

variation. *Computational Statistics & Data Analysis*, 124:117–131.

Patterson, H. D. and Thompson, R. (1971). Recovery of inter-block information when block sizes

are unequal. *Biometrika*, 58:545–554.

Pilavakis, D., Paparoditis, E., and Sapatinas, T. (2019). Moving block and tapered block bootstrap

for functional time series with an application to the k-sample mean problem. *Bernoulli*, 25:3496–

3526.

Pinheiro, J. and Bates, D. (2000). *Mixed-Effects Models in S and S-PLUS*. Statistics and

Computing. Springer.

Reluga, K., Lombardía, M.-J., and Sperlich, S. (2024). Bootstrap-based statistical inference

for linear mixed effects under misspecifications. *Computational Statistics & Data Analysis*,

199:108014.

Samanta, M. and Welsh, A. (2013). Bootstrapping for highly unbalanced clustered data. *Compu-*

*tational Statistics & Data Analysis*, 59:70–81.

Shao, J., Kübler, J., and Pigeot, I. (2000). Consistency of the bootstrap procedure in individual

bioequivalence. *Biometrika*, 87:573–585.